

# Analyses of Mlc–EIIB<sup>Glc</sup> interaction and a plausible molecular mechanism of Mlc inactivation by membrane sequestration

Tae-Wook Nam\*, Ha Il Jung<sup>††</sup>, Young Jun An<sup>††</sup>, Young-Ha Park\*, Sang Hee Lee<sup>‡</sup>, Yeong-Jae Seok<sup>\*§</sup>, and Sun-Shin Cha<sup>†§</sup>

\*Department of Biological Sciences and Institute of Microbiology, Seoul National University, Seoul 151-742, Korea; <sup>†</sup>Marine Biotechnology Center, Korea Ocean Research and Development Institute, Ansan 426-744, Korea; and <sup>‡</sup>Department of Biological Sciences, Myongji University, Yongin 449-728, Korea

Edited by Winfried Boos, University of Konstanz, Konstanz, Germany, and accepted by the Editorial Board January 22, 2008 (received for review September 30, 2007)

In *Escherichia coli*, glucose-dependent transcriptional induction of genes encoding a variety of sugar-metabolizing enzymes and transport systems is mediated by the phosphorylation state-dependent interaction of membrane-bound enzyme EIIB<sup>Glc</sup> (EIIB<sup>Glc</sup>) with the global repressor Mlc. Here we report the crystal structure of a tetrameric Mlc in a complex with four molecules of enzyme EIIB<sup>Glc</sup> (EIIB), the cytoplasmic domain of EIIB<sup>Glc</sup>. Each monomer of Mlc has one bound EIIB molecule, indicating the 1:1 stoichiometry. The detailed view of the interface, along with the high-resolution structure of EIIB containing a sulfate ion at the phosphorylation site, suggests that the phosphorylation-induced steric hindrance and disturbance of polar intermolecular interactions impede complex formation. Furthermore, we reveal that Mlc possesses a built-in flexibility for the structural adaptation to its target DNA and that interaction of Mlc with EIIB fused only to dimeric proteins resulted in the loss of its DNA binding ability, suggesting that flexibility of the Mlc structure is indispensable for its DNA binding.

enzyme EIIB<sup>Glc</sup> | glucose signaling | protein–protein interaction | transcription regulation

Bacteria sense continuous changes in their environment and adapt metabolically to compete effectively with other organisms for limiting nutrients. One sensory transduction system monitoring availability of a certain group of carbon sources is the phosphoenolpyruvate:sugar phosphotransferase system (PTS) (1). In addition to concomitant transport and phosphorylation of sugars, PTSs take part in a variety of physiological processes through direct interactions with their target proteins (2–5).

It is a normal occurrence that cells make more proteins necessary to transport and metabolize PTS sugars when they encounter an environment where PTS sugars are available. Glucose, a representative PTS sugar, mediates transcriptional activation of several genes for PTS-related sugar transporters and some enzymes involved in glycolysis (1, 6). Mlc, a tetrameric protein (7), is a signaling mediator for glucose induction of several PTS operons and related genes (8–14).

A unique feature of induction of the Mlc regulon by glucose is that the effector molecule modulating Mlc activity is a membrane-bound protein, EIIB<sup>Glc</sup> (7, 15, 16), in which cytosolic EIIB protein is attached to membrane-embedded EII<sub>C</sub> protein through a linker of >20 aa. In the absence of glucose, EIIB<sup>Glc</sup> mainly exists in the phosphorylated form (pEIIB<sup>Glc</sup>). Because Mlc cannot interact with pEIIB<sup>Glc</sup>, Mlc dissociates from pEIIB<sup>Glc</sup> to bind to target promoters and repress their transcription. When glucose is available, transported glucose takes the phospho-groups away from pEIIB<sup>Glc</sup> and the dephosphorylated EIIB<sup>Glc</sup> recruits Mlc to sequester it from its target promoters. This leads to increased synthesis of EIIB<sup>Glc</sup> and other PTS proteins necessary to take up and metabolize glucose more efficiently.

The physiological importance of the glucose-specific enzyme II and the discovery of this regulatory circuit led to structural studies

about dephosphorylated EIIB (17, 18) and an Mlc mutant (19). However, the underlying mechanisms of how the phosphorylation of EIIB<sup>Glc</sup> affects the interaction with Mlc and why Mlc loses its DNA-binding activity when localized to the membrane still remain unexplained. To address these questions, we determined the crystal structures of the Mlc/EIIB complex and sulfo-EIIB (S-EIIB) mimicking the phosphorylated state.

## Results and Discussion

**Structure of Mlc in the Complex.** We obtained crystals of the Mlc/EIIB complex containing two Mlc monomers and two bound EIIB molecules in an asymmetric unit. The structure of the complex was determined by molecular replacement and refined to 2.85-Å resolution [see supporting information (SI) Table 1]. An Mlc monomer is composed of three domains playing distinct roles: a DNA-binding domain (D-domain), an EIIB-binding domain (E-domain), and an oligomerization domain (O-domain) (Fig. 1A). Residues 1 to 81 and 395 to 406 adopt a compact globular D-domain composed of four helices. Among them,  $\alpha_2$  and  $\alpha_3$  constitute a classical helix–turn–helix (HTH) DNA-binding motif. In this classical motif,  $\alpha_3$ , often called a “recognition helix,” makes specific contacts with bases in the major groove of DNA. Residues 82 to 194 and 381 to 394 constitute a three-layered structure of E-domain. A central sheet consisting of five strands is flanked by three  $\alpha$ -helices and two short  $\beta$ -strands. Residues 195–380 form O-domain with a four-stranded sheet sandwiched asymmetrically by eight  $\alpha$ -helices on one face and by one  $\alpha$ -helix on the other face and contains a zinc ion known to play a structural role (19).

Each domain structure of one Mlc monomer is virtually identical to that of another monomer in an asymmetric unit. However, structural comparison between the two Mlc monomers shows that the position of D- and E-domains with respect to O-domain is not fixed, indicating that Mlc has a hinge between E- and O-domains (Fig. 1B). The flexible connection loop and the weak interdomain contact between E- and O-domains support the innate flexibility at the hinge.

The lateral face of O-domain from a monomer makes contact with the same region of an adjacent monomer in an asymmetric

Author contributions: T.-W.N., H.I.J., and Y.J.A. contributed equally to this work; Y.-J.S. and S.-S.C. designed research; T.-W.N., H.I.J., Y.J.A., and Y.-H.P. performed research; S.H.L. contributed new reagents/analytic tools; T.-W.N., Y.-J.S., and S.-S.C. analyzed data; and Y.-J.S. and S.-S.C. wrote the paper.

The authors declare no conflict of interest.

This article is a PNAS Direct Submission. W.B. is a guest editor invited by the Editorial Board.

Data deposition: The atomic coordinates of the Mlc/EIIB complex and the S-EIIB protein have been deposited in the Protein Data Bank, www.pdb.org (PDB ID codes 3BP8 and 3BP3, respectively).

<sup>§</sup>To whom correspondence may be addressed. E-mail: yjseok@snu.ac.kr or chajung@kordi.re.kr.

This article contains supporting information online at [www.pnas.org/cgi/content/full/0709295105/DC1](http://www.pnas.org/cgi/content/full/0709295105/DC1).

© 2008 by The National Academy of Sciences of the USA

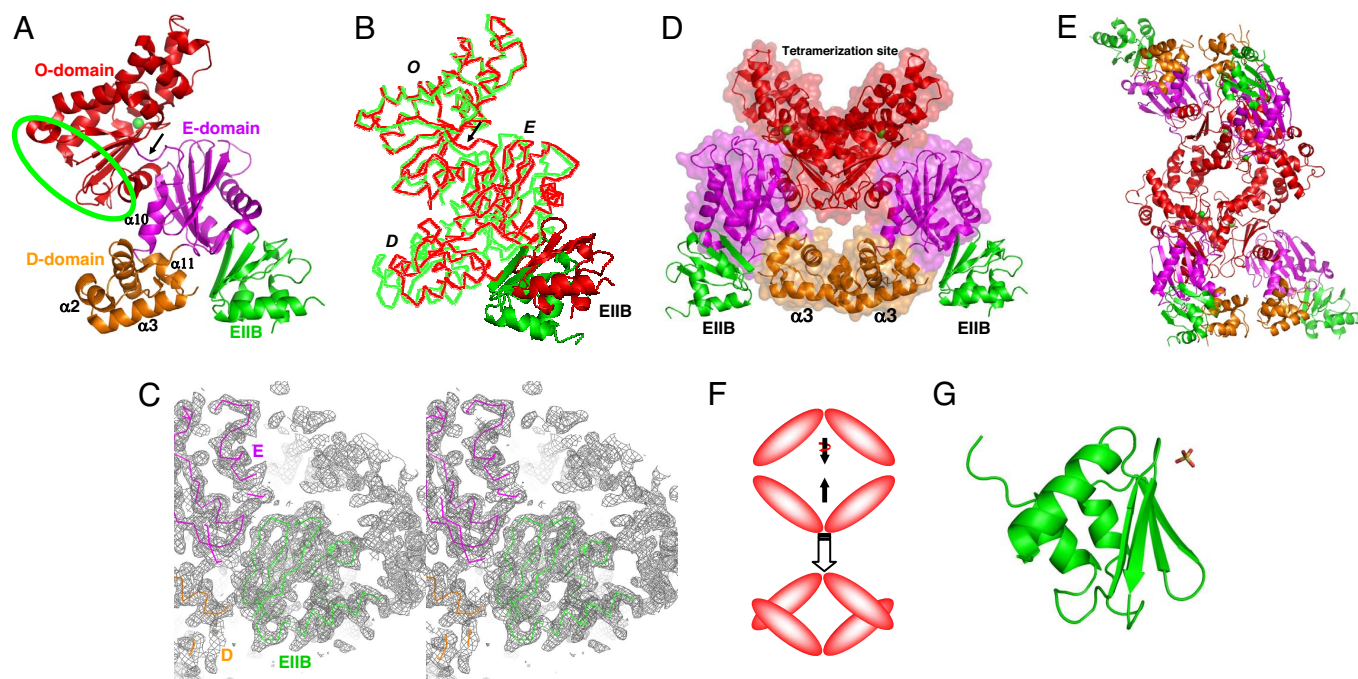


**Fig. 1.** Structures of Mlc/EIIB and S-EIIB. (A) Ribbon diagram of an Mlc monomer with one bound EIIB molecule. D-, E-, and O-domains in Mlc are colored in orange, magenta, and red, respectively. EIIB is colored in green. This color scheme of Mlc and EIIB is maintained in all figures. A green ellipsoid indicates the dimerization site. A zinc ion in O-domain is represented by a green sphere in all figures. A black arrow indicates the hinge region between E- and O-domains. (B) C $\alpha$  tracing of superposed Mlc monomers. A black arrow indicates the hinge region between E- and O-domains. For clarity, EIIB is represented by a ribbon diagram. D, E, and O refer to D-, E-, and O-domains in all figures. (C) A simulated annealing 2F<sub>o</sub>-F<sub>c</sub> omit map contoured at 1 $\sigma$ . At a refinement stage with an R value of 23.7%, the structure was disturbed at 1,000 K with the omission of EIIB molecules and the residues within 3.5 Å from EIIB molecules, and then the map was calculated with the same omission. (D) Ribbon diagram of an Mlc dimer with two bound EIIB molecules in green. (E) Ribbon diagram of an Mlc tetramer with four bound EIIB molecules. (F) Schematic drawing describing the tetramerization mode of Mlc. For clarity, only O-domains are shown. (G) Ribbon diagram of EIIB. A sulfate ion is represented by a stick.

unit, locating two monomers side by side (Fig. 1D). In this dimeric conformation, two recognition helices of Mlc are close to each other, which appears to be consistent with an interaction with a palindromic target. According to size-exclusion chromatography, Mlc behaved as a tetramer regardless of the presence of EIIB, indicating that Mlc keeps its tetrameric conformation upon complex formation (data not shown). Thus we searched for the tetrameric contact in crystals and found that the upper part of an Mlc dimer with the shape of  $\nabla$  makes geometric packing interactions with the same part of a symmetry-related Mlc dimer with the shape of  $\wedge$  (Fig. 1E). The  $\approx 45^\circ$  rotational stacking of an Mlc dimer with respect to a contacting dimer allows such a clasping intermolecular contact as  $\nabla$  and  $\wedge$  overlapping (Fig. 1F). This clasping dimer-dimer contact excludes 2,008 Å<sup>2</sup> of solvent-accessible surface area, of which 71% is hydrophobic surface.

The uncomplexed R52H mutant structure of Mlc (19) allows us to investigate the structural alteration of Mlc upon complex formation. Structural superposition shows that D-, E-, and O-domains of Mlc in the complex are virtually identical to those of the Mlc mutant, respectively; the rms deviations of superposed C $\alpha$  atoms are within 0.5 Å. The dimerization mode is also identical in the two Mlc structures. In addition, the mutant structure also has a hinge region between E- and O-domains just like Mlc in the complex. In summary, Mlc appears to undergo no conformational changes upon complex formation.

One remarkable difference between the two Mlc structures is the tetrameric conformation. We observed a clasping dimer-dimer contact between two Mlc dimers in complex crystals, which generates a tetramer. However, in the previous mutant structure, there is no equivalent clasping tetrameric contact. Instead, the upper part of an Mlc dimer makes a simple edge-to-edge contact with the same part of another dimer in the mutant structure. To verify the clasping

tetrameric conformation, we designed an Mlc mutant harboring two point mutations (Arg306Gly and Leu310Gly) to examine whether the disturbance of the clasping tetrameric contact results in Mlc dimerization. The two mutation sites were selected because the interaction between Arg-306 in a dimer and a concaved hydrophobic surface containing Leu-310 in another dimer (SI Fig. 5) represents the geometric complementarity of the tetrameric contact. In gel filtration experiments, the mutant protein was eluted as a dimeric form whereas the wild-type protein was eluted as a tetrameric form (SI Fig. 6). This mutational study, together with the crucial importance of geometric complementarity in the molecular interaction (20), strongly suggests that the clasping tetrameric conformation is more likely to be physiologically relevant rather than the simple edge-to-edge tetrameric contact.

Previously, it has been reported that the deletion of C-terminal 18 residues leads to Mlc dimerization (21). The dimerization appears to be related to the structural instability of the mutant protein. It has been shown that mutations of residues that coordinate a zinc ion in O-domain disturb the DNA-binding activity of Mlc (19). The D-domain of Mlc, which is responsible for DNA binding, is far away from O-domain (Fig. 1A). Therefore, the loss of DNA-binding activity of the zinc-depleted Mlc mutants indicates that the structural instability of O-domain remotely affects the structure of D-domain in some way. Similarly, it can be assumed that the structural disturbance of D- or E-domain can also remotely alter the structure of O-domain. The C-terminal 18 residues span two C-terminal helices ( $\alpha 10$  and  $\alpha 11$ ) that are important for the proper folding of D- and E-domains, respectively (Fig. 1A). The  $\alpha 10$  helix is the only helix covering one surface of the central sheet of E-domain. Therefore, the deletion of  $\alpha 10$  means the break of the three-layered  $\alpha/\beta$  sandwich fold of E-domain, which could make E-domain unstable. The  $\alpha 11$  helix is the fourth helix of D-domain.



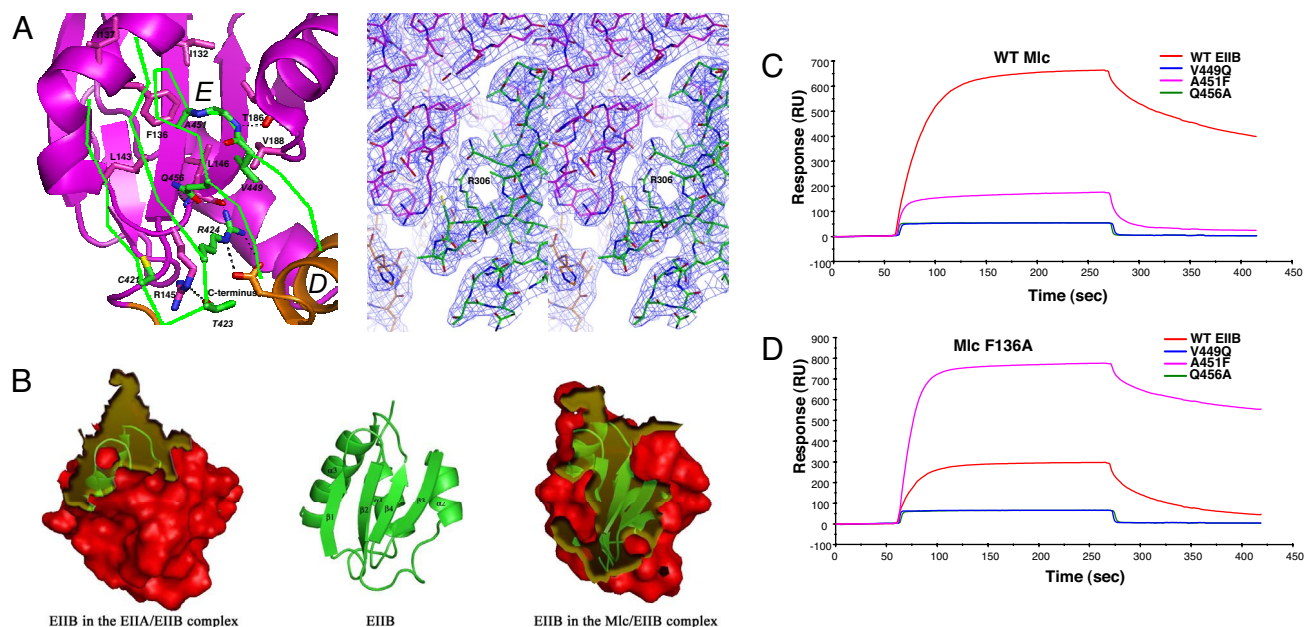


**Fig. 2.** Binding interface and residues involved in intermolecular interactions. (A Left) Close-up view of binding interface. Mlc is represented by a ribbon drawing, but, for clarity, only C $\alpha$  tracing of the sheet of EIIB implicated in complex formation is shown. To distinguish between residues of Mlc and EIIB, residues of EIIB are labeled by italic type. (A Right) Final  $2F_o - F_c$  electron density map contoured at  $1\sigma$  showing the interface region around Arg-324 of EIIB. Oxygen, sulfur, and nitrogen are shown in red, yellow, and blue, respectively, in all figures. Dashed lines indicate polar intermolecular interactions. (B) Surface representation of EIIBs in the EIIA/EIIB complex and the Mlc/EIIB complex. The transparent yellow regions indicate binding interfaces in the two complexes. The central ribbon diagram is presented as a reference showing the secondary structure elements. (C and D) SPR analyses of the interaction between EIIB and Mlc. Wild type and mutants of EIIB were separately immobilized onto the surface of a CM5 sensor chip by amide coupling as indicated, and wild type (C) and F136A mutant Mlc (D) were injected to measure real-time interactions. Proteins were exposed for 3.5 min at 112.8 nM.

Leu-400 and Leu-404 in  $\alpha 11$  form a hydrophobic core with hydrophobic residues from three other helices (figure not shown). The removal of  $\alpha 11$ , therefore, would disrupt the core structure of D-domain. Consequently, the C-terminal deletion destabilizes the structures of D- and E-domains, and the structural instability of D- and E-domains would remotely affect the structure of O-domain, leading to Mlc dimerization. In addition, the inability of the deletion mutant to bind EIIB can also be related to the structural disturbance of D- and E-domains because E-domain and the C terminus of D-domain (Fig. 2A) are in charge of EIIB binding.

#### Structure of EIIB in the Complex and Interface of the Mlc/EIIB Complex.

EIIB adopts a simple  $\alpha/\beta$  fold. A four-stranded antiparallel  $\beta$ -sheet is packed with three helices on one face, and the other face of the sheet is fully exposed to solvent (Fig. 1G). The rms deviation of C $\alpha$  atoms of EIIB structure in the complex and a previous solution structure of EIIB (Protein Data Bank ID code 1O2F) (18) is only 0.37 Å. This minute structural disparity shows that the solution structure is by far and away the most accurate NMR structure determined so far and that EIIB is a very tightly packed structure that is not affected by complex formation.

Mlc and EIIB form a complex with the 1:1 stoichiometry. The solvent-exposed face of the sheet in EIIB binds mainly to E-domain of Mlc, which confirms that EIIB domain is enough for the interaction with Mlc (7). The average B-factor of two EIIB molecules (42.78 Å<sup>2</sup>) is similar to those of their interacting E-domains (40.19 Å<sup>2</sup>), and the occupancy refinement revealed that the occupancy of EIIB molecules (0.985) is comparable to that of Mlc molecules (0.988). These, together with the simulated annealed omit map (Fig. 1C), prove the presence of EIIB molecule in the complex crystals. The binding interface can be divided into two areas: an upper contact region and a lower contact region (Fig. 2A). The upper contact region is located in the hydrophobic concaved region of E-domain in Mlc. The backbone of residues 448–453 and

the side chains of Val-449 and Ala-451 in EIIB form a tight contact with the hydrophobic region of Mlc lined by Ile-132, Phe-136, Ile-137, Leu-143, Leu-146, Thr-186, and Val-188. The only possible polar contact here may be interactions between backbone atoms of Val-450 in EIIB and Thr-186 in Mlc that are within 3 Å. The lower contact region is located at the boundary between D- and E-domains of Mlc. In contrast to the hydrophobic nature in the upper contact region, polar interactions are dominant in this interface. The side chains of Thr-423 and Gln-456 in EIIB could make hydrogen bonds with the guanidino group of Arg-145 and the amide nitrogen of Leu-146 in Mlc, respectively. It is noteworthy that the guanidino group of Arg-424 in EIIB, which was previously identified as a critical residue in binding to Mlc (21), is located in the vicinity of the carbonyl oxygen of Leu-146 and the C-terminal carboxylate<sup>†</sup> in Mlc, indicating multiple polar interactions. Interestingly, Cys-421 of EIIB, the phosphorylation site, is >5 Å away from Mlc in the Mlc/EIIB structure, making no direct contact with Mlc. This is consistent with a previous study noting that Cys-421 is not necessary for the interaction between Mlc and EIIB (21).

EIIB interacts with two proteins, EIIA and Mlc. Interestingly, the contact regions of EIIB for Mlc and EIIA are only partially overlapped. The investigation of the buried surface area of EIIB in the EIIA/EIIB and Mlc/EIIB complexes clearly shows that  $\beta 3$ ,  $\beta 4$ , and the  $\beta 3$ – $\beta 4$  turn mainly contribute to the complex formation with Mlc whereas the convexed region composed of the  $\beta 1$ – $\beta 2$  turn region (residues 419–426), the connecting loop between  $\beta 4$  and  $\alpha 3$ , and the N-terminus of  $\alpha 3$  is mainly implicated in the complex formation with EIIA (Fig. 2B). Only residues 423–424 play roles in the formation of both complexes.

The minimal overlapping of contacting regions in EIIB is a neatly

<sup>†</sup>Very recently, the C-terminal amino acid (Gly406) of Mlc has been revealed to be involved in interacting with EIIB (26), which gives experimental support to our observation.

**Table 1. Kinetic parameters for the interaction of wild-type or F136A mutant Mlc with wild-type or A451F mutant EII<sub>B</sub>**

Interaction	$k_{a_r}$ , 1/Ms	$k_{d_r}$ , 1/s	$K_A$	$K_D$
Wild-type E1B and wild-type M1c	$(9.95 \pm 1.71) \times 10^5$	$(3.85 \pm 0.77) \times 10^{-3}$	$(2.60 \pm 0.77) \times 10^8$	$(4.14 \pm 1.22) \times 10^{-9}$
Wild-type E1B and M1c (F136A)	$(9.66 \pm 1.75) \times 10^5$	$(1.30 \pm 0.14) \times 10^{-2}$	$(7.47 \pm 1.18) \times 10^7$	$(1.37 \pm 0.22) \times 10^{-8}$
E1B (A451F) and wild-type M1c	$(7.76 \pm 1.53) \times 10^5$	$(8.79 \pm 1.79) \times 10^{-3}$	$(9.25 \pm 3.05) \times 10^7$	$(1.17 \pm 0.35) \times 10^{-8}$
E1B (A451F) and M1c (F136A)	$(2.04 \pm 0.23) \times 10^6$	$(2.25 \pm 0.48) \times 10^{-3}$	$(9.47 \pm 2.53) \times 10^8$	$(1.12 \pm 0.27) \times 10^{-9}$

Data were collected from five to seven independent SPR analyses by injecting various concentrations of Mlc proteins over the surfaces immobilized with E11B proteins.

designed tool to run the regulatory circuit of the Mlc regulon. In the Mlc/EIIB complex, most EIIB-contacting residues including Cys-421 of EIIB are exposed to solvent. This may allow the phosphorylated EIIB to access EIIB in the complex with Mlc and thus to transfer a phosphate group to EIIB. The phosphorylation of EIIB makes Mlc dissociate from P-EIIB and bind to its target operators.

Based on the complex structure, we have used surface plasmon resonance (SPR) spectroscopy to validate the significance of newly identified residues at the complex interface (Val-449 in the upper contact region and Gln-456 in the lower contact region on EIIB) for the formation of the stable complex with Mlc. Wild-type and mutant EIIB proteins were immobilized onto the carboxymethylated dextran surface of a CM5 sensor chip by using the standard amine coupling chemistry (7, 22, 23). When wild-type Mlc was allowed to flow over the immobilized EIIB, high-affinity interaction was detectable as expected from our previous report (Fig. 2 *C* and *D* and Table 1) (7). When the Mlc protein was exposed to surfaces immobilized with the V449Q and Q456A mutants of EIIB, however, interaction was hardly detectable (Fig. 2*C*). In the hydrophobic upper contact region, the small side chain of Ala-451 in EIIB and the bulky side chain of Phe-136 in Mlc constitute the best-fitted pair representing a complementary aspect of the contact between the two proteins (Fig. 2*A*). This complementarity between Ala-451 of EIIB and Phe-136 of Mlc was also verified by employing SPR spectroscopy after site-directed mutagenesis. Either when Ala-451 of EIIB was mutated to Phe or when Phe-136 in Mlc was changed to Ala, the complex showed much weaker association than the wild-type pair (Fig. 2 *C* and *D* and Table 1). As expected, when the F136A mutant of Mlc was introduced over the CM5 surface immobilized with the A451F mutant of EIIB, high-affinity interaction was recovered to the level of the wild-type pair (Fig. 2*D*), confirming the validity of our complex model. It should be noted that the F136A mutant of Mlc showed no detectable interaction with V449Q and Q456A mutants of EIIB (Fig. 2*D*).

**Structural Basis Elucidating How the Phosphorylation of EIIB Prevents It from Binding to Mlc.** In the structure of S-EIIB determined at 1.65-Å resolution, a sulfate ion exists beside Cys-421, the phosphorylation site of EIIB, interacting with three amide nitrogens of residues 422–424 and the side chains of Cys-421 and Arg-424 (Figs. 1*G* and 3). In this configuration, the sulfhydryl group of Cys-421 is within 3 Å from the sulfur atom of the sulfate ion, showing that Cys-421 is ready for nucleophilic attack on the sulfur atom. Because a sulfate ion is the structural homologue of a phosphate ion, this structure provides information on the phosphorylated EIIB (P-EIIB).

The structure of S-EIIB and the superposition of the structure of S-EIIB onto that of EIIB in the Mlc/EIIB complex provide insights into the phosphorylation state-dependent interaction of EIIB with Mlc. One remarkable difference between EIIB in a complex with Mlc and S-EIIB is the side chain conformation of Arg-424, which makes several intermolecular interactions with Mlc on complex formation (Fig. 2A). In EIIB complexed with Mlc the side chain chi-angles of Arg-424 are  $-58.5^\circ$ ,  $171.3^\circ$ ,  $-59.4^\circ$ ,  $176.2^\circ$ , and  $180^\circ$ , whereas those of Arg-424 in S-EIIB are  $-67.3^\circ$ ,  $-73^\circ$ ,  $177.7^\circ$ ,  $61.3^\circ$ , and  $-179.6^\circ$ , indicating that the side chain of Arg-424 in S-EIIB should undergo considerable torsional changes to assume the same

side chain conformation as that of Arg-424 in EIIB complexed with Mlc. However, such torsional change of Arg-424 in S-EIIB is impossible because of the tight binding of the side chain of Arg-424 to the sulfate. The interaction between the sulfate ion and Arg-424 in S-EIIB reflects the intramolecular interaction between the phosphate moiety at Cys-421 and Arg-424 in P-EIIB. Therefore, the fixed side chain of Arg-424 to the phosphate moiety in P-EIIB could not protrude toward Mlc, which would prevent the formation of intermolecular interactions between Arg-424 of EIIB and Mlc. The fact that the R424A point mutation makes EIIB incapable of binding to Mlc proves the essential role of Arg-424-mediated intermolecular interactions for the complex formation (21). The inability of P-EIIB to make Arg-424-mediated intermolecular interactions is thus the cause of the inability of P-EIIB to bind to Mlc. In addition, according to the structural superposition (Fig. 3), the fixed side chain of Arg-424 to the sulfate ion in S-EIIB is only 0.5 Å away from the backbone of residues 144–145 to induce steric hindrance. In conclusion, both the loss of critical intermolecular interactions mediated by Arg-424 and steric hindrance, which are instigated by the phosphorylation of EIIB, trigger the dissociation of Mlc from pEIIB<sup>Gle</sup> *in vivo*.

**The Structural Flexibility of Mlc Is Essential for Its DNA-Binding Activity and for Its Regulation.** Two linearly located recognition helices with  $\approx 25$ -Å center-to-center distance in an Mlc dimer superficially appear to be adequate for their fitting into two tandem major grooves of DNA (Fig. 44). According to the DNA-complexed structure of BlaI, whose HTH motif is structurally similar to that of Mlc (SI Fig. 7), however, two recognition helices from two HTH motifs in BlaI, which are in two major grooves of

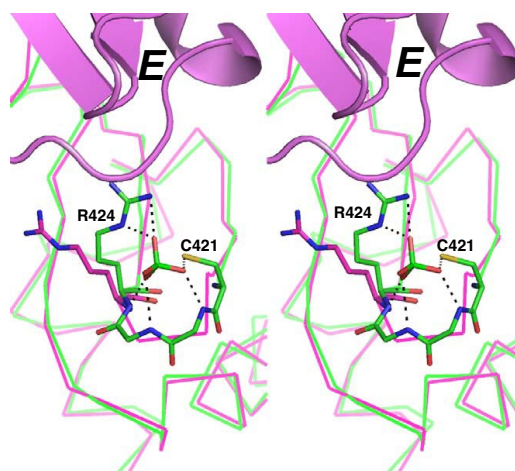
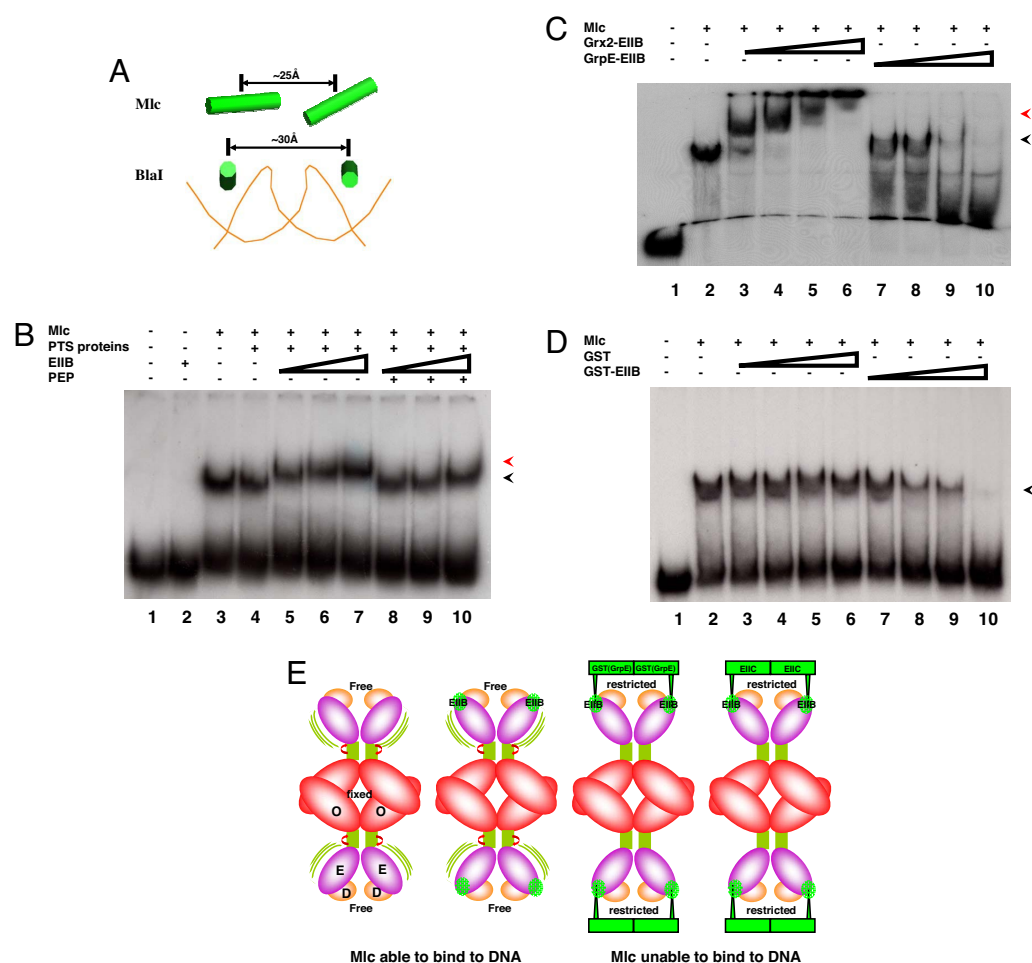


**Fig. 3.** Stereo view of the local environment around Cys-421. The structure of S-ElIB is superposed onto that of ElIB in the complex structure for this figure. Mlc is represented by a ribbon drawing, but, for clarity, only C $\alpha$  tracing of the sheet of ElIB implicated in complex formation is shown. ElIB in the complex structure and S-ElIB are colored in violet and green, respectively. In ElIB bound to Mlc, only Arg-424 is shown for clarity. Dotted lines represent polar interactions between the bound sulfate ion and ElIB.



**Fig. 4.** Plausible mechanism for the loss of DNA-binding ability of Mlc. (A) Spatial arrangement of two recognition helices ( $\alpha 3$ ) represented by cylinders in Mlc and BlaI. For clarity, only phosphate backbone of DNA in the complex structure between BlaI and DNA (Protein Data Bank ID code 1XSD) is shown. (B) Electrophoretic mobility-shift assays showing that the Mlc/EIIB complex efficiently binds to the Mlc target site.  $^{32}$ P-labeled DNA fragments (17 nM) covering the Mlc binding region of the *ptsG* promoter (from -260 to -155 with respect to the transcriptional start site) were mixed with 0.45  $\mu$ M Mlc. A total of 1  $\mu$ M enzyme I and 1.4  $\mu$ M HPr and enzyme IIA<sup>Glc</sup> were added as PTS proteins as indicated. EIIB was at 2  $\mu$ M (lanes 5 and 8), 4  $\mu$ M (lanes 6 and 9), and 8  $\mu$ M (lanes 2, 7, and 10). The phosphorylated form of EIIB was generated by adding 5 mM PEP to the reaction mixture (lanes 8–10). The black arrowhead indicates the Mlc-bound DNA, and the red arrowhead shows the binding of the Mlc/EIIB complex to DNA. (C) Effects of Grx2-EIIB and GrpE-EIIB fusion proteins on Mlc binding to its target DNA.  $^{32}$ P-labeled DNA probe was mixed with Mlc as described in B, and Grx2-EIIB or GrpE-EIIB was added to the reaction mixture. Grx2-EIIB and GrpE-EIIB were at 0.31  $\mu$ M (lanes 3 and 7), 0.62  $\mu$ M (lanes 4 and 8), 1.25  $\mu$ M (lanes 5 and 9), and 2.5  $\mu$ M (lanes 6 and 10). The black arrowhead indicates Mlc-bound DNA, and the red arrowhead points to the binding of the Mlc/Grx2-EIIB complex to DNA. (D) Inhibition of Mlc binding to its target DNA by the GST-EIIB fusion protein.  $^{32}$ P-labeled DNA probe was mixed with Mlc as described in B, and GST or GST-EIIB was added to the reaction mixture. GST was at 0.44  $\mu$ M (lane 3), 0.88  $\mu$ M (lane 4), 1.76  $\mu$ M (lane 5), and 3.52  $\mu$ M (lane 6), and GST-EIIB was at 0.31  $\mu$ M (lane 7), 0.62  $\mu$ M (lane 8), 1.25  $\mu$ M (lane 9), and 2.5  $\mu$ M (lane 10). The arrow indicates the protein/DNA complexes. (E) Schematic drawing describing the structural freedom around the hinge region of free and EIIB-bound Mlc and the restricted structural freedom around the hinge region of Mlc bound to GST(GrpE)-EIIB and EIICB<sup>Glc</sup>. Green bars represent the hinge regions between E- and O-domains.



DNA, adopt a different arrangement; they are parallel to each other with a gap of  $\approx 30$  Å (Fig. 4A). Although the detailed interaction between HTH motifs of BlaI and DNA should be different from that between HTH motifs of Mlc and DNA, the DNA complex structure provides insights into the overall arrangement of two recognition helices, which can nestle in DNA major grooves because DNA adopts a common structure regardless of sequences. In this regard, the spatial arrangement of two recognition helices observed in our structure is not suitable for their nestling in tandem major grooves of DNA despite their close positioning (Fig. 4A). Nevertheless, Mlc efficiently binds to DNA, indicating a rearrangement of HTH motifs in Mlc upon DNA binding. The hinge of Mlc whose structural freedom is not affected by EIIB binding (Fig. 1B) may allow such a structural adaptation because a hinge is the very region that accommodates conformational changes in proteins.

The retarded mobility of DNA by Mlc in the presence of EIIB (Fig. 4B) ascertains that EIIB binding alone has no effect on both the structure and DNA-binding activity of Mlc, and the membrane localization exerts an essential role in preventing Mlc from binding to DNA *in vivo* (24). It should be noted that dephosphorylated EIIB but not P-EIIB supershifted the Mlc-bound target sequence in the *ptsG* promoter (Fig. 4B), meaning that EIIB still interacts with Mlc without affecting its DNA-binding activity, whereas P-EIIB even

cannot interact with Mlc as shown before (7). Then, a question remains as to why Mlc loses its DNA-binding ability when localized to the membrane. The direct interaction between hydrophobic membrane and soluble Mlc is not energetically favorable. In addition, the existence of the long linker between cytosolic EIIB and membrane-embedded EIIC and the absence of direct interaction between Mlc and EIIC indicate that EIIB-bound Mlc is located some distance away from membrane. The lower possibility of interactions between Mlc and the membrane led us to assume that the restriction of the structure flexibility of Mlc set by membrane localization might be responsible for the loss of its DNA-binding activity.

The innate flexibility at the hinge allows the adjustment of the spatial arrangement of HTH motifs in Mlc to that of major grooves in DNA, conferring the DNA-binding ability of Mlc. However, when Mlc is attached to the membrane through interactions with EIICB<sup>Glc</sup> the four ends of Mlc must be fixed on the membrane. The anchoring of four ends to the membrane should significantly restrict the freedom in the domain arrangement of Mlc (Fig. 4E), preventing the essential induced fit of Mlc for DNA binding. Consequently, the sequestered Mlc cannot bind its target promoters. According to this model, the structural restriction generated by the anchoring of Mlc to the membrane is the key determinant for Mlc inactivation.

If this is the case, any kind of structural restriction hindering the domain arrangement of Mlc would inhibit binding of Mlc to its target DNA. To prove this, we prepared chimeric proteins in which EIIB was fused to cytosolic proteins in *Escherichia coli*: two dimeric proteins, GST (monomer is  $\approx 22.9$  kDa) and GrpE (monomer is  $\approx 21.8$  kDa), and one monomeric protein, Grx2 ( $\approx 24.3$  kDa), a GST-like glutaredoxin having a high degree of structural similarity and similar size with GST (25). In our structure, the N-terminal 12 residues of EIIB are disordered, which indicates that a long flexible loop exists between EIIB and fused proteins in these chimeric proteins. Therefore, it is not likely that these proteins physically mask D-domains when associated with Mlc. Instead, the conformational freedom of Mlc would be considerably confined by the oligomeric state of EIIB-fused proteins that bind Mlc because Mlc anchored to the membrane is structurally restricted. The purified monomeric Grx2-EIIB construct produced a supershifted complex with DNA and Mlc, meaning that this construct did not induce the conformational change of Mlc to disassociate it from DNA (Fig. 4C, lanes 3–6). Intriguingly, however, EIIB fused to the C terminus of GST having a high degree of structural similarity and similar size with Grx2 efficiently prevented the association of Mlc to DNA (Fig. 4D), showing that the structural restriction put by a cytosolic protein also makes Mlc inactive. Similarly, EIIB fused to another well known homodimeric protein, GrpE, also dissociated Mlc from its target DNA sequence (Fig. 4C, lanes 7–10). The chimeric EIIB proteins can be phosphorylated by the PTS and show the phosphorylation state-dependent interaction with Mlc (SI Fig. 8). These indicate that EIIB fused to a dimeric cytosolic protein can efficiently regulate Mlc, as does EIIB fused to a membrane-embedded EIIC. It should be noted, however, that EIIB fused to GST and Grx2 showed negative effects on the PTS expression, as did GST and Grx2 themselves (data not shown). Therefore, we could not reproduce the *in vitro* effects of these chimeric EIIB fusion constructs on the *ptsG* transcription *in vivo*. An inactivation model of Mlc has been proposed in which the direct interaction of the membrane-localized Mlc with membrane may induce the dimerization of Mlc (24). However, the dimerization cannot be respon-

sible for Mlc inactivation in that Mlc complexed with EIIB or GST-EIIB complex keeps tetrameric conformation (data not shown) and that a dimeric mutant of Mlc still binds DNA (SI Fig. 9). In conclusion, our experiments with EIIB chimeras indicate that the restriction of conformational freedom resulting from the anchoring of four ends of Mlc to the membrane could be the primary cause of its loss of DNA-binding activity *in vivo* (Fig. 4E).

## Materials and Methods

**Purification.** Cloning is described in *SI Materials and Methods*. Expression and purification of EIIB proteins and wild-type and mutant Mlc proteins with a single amino acid change were performed as described previously (7, 12). Whereas wild-type and mutant Mlc proteins with a single amino acid change were insoluble in 10 mM Tris-HCl buffer (pH 7.5) containing 1 mM DTT, Mlc harboring two point mutations (Arg306Gly and Leu310Gly) at O-domain was soluble at neutral pH. Therefore, after sonication, the crude extract of cells overproducing this mutant was loaded on a Q Sepharose Fast Flow column (Amersham Pharmacia Biotech) and eluted with a 0–1.0 M NaCl gradient in the Tris buffer. Eluted fractions containing the mutant were concentrated and loaded onto a Superdex 200 HR16/60 column (Amersham Pharmacia Biotech).

**Crystallization.** Crystals of Mlc/EIIB and S-EIIB were obtained by the batch crystallization method. Crystallization conditions are described in *SI Materials and Methods*.

**Structure Determination and Refinement.** The molecular replacement, model building, and refinement were performed by using MolRep, XtalView, and CNS, respectively. The full procedure is described in *SI Materials and Methods*.

**Surface Plasmon Resonance Spectroscopy.** SPR experiments were performed on a BIAcore 3000 instrument (Biacore AB). The full method is described in *SI Materials and Methods*.

**Gel Shift Assays.** Gel shift assays were carried out as described previously (7).

**ACKNOWLEDGMENTS.** S.-S.C. was supported by a grant from the Functional Proteomics Center, the 21C Frontier Research and Development Program of the Ministry of Science and Technology of Korea (FPR06B2-140), and in part by a grant from the National Institute of Health of Korea Centers for Disease Control and Prevention. Y.-J.S. was supported by Korea Research Foundation Grant KRF-2004-015-C00480 and Korea Science and Engineering Foundation Grant R01-2005-000-10038-0 funded by the Ministry of Science and Technology of Korea.

- Postma PW, Lengeler JW, Jacobson GR (1993) Phosphoenolpyruvate:carbohydrate phosphotransferase systems of bacteria. *Microbiol Rev* 57:543–594.
- Lee C-R, et al. (2005) Requirement of the dephospho-form of enzyme IIA<sup>Ntr</sup> for derepression of *Escherichia coli* K-12 *ilvBN* expression. *Mol Microbiol* 58:334–344.
- Deutscher J, Francke C, Postma PW (2006) How phosphotransferase system-related protein phosphorylation regulates carbohydrate metabolism in bacteria. *Microbiol Mol Biol Rev* 70:939–1031.
- Park Y-H, Lee BR, Seok Y-J, Peterkofsky A (2006) In vitro reconstitution of catabolite repression in *Escherichia coli*. *J Biol Chem* 281:6448–6454.
- Lee C-R, Cho S-H, Yoon M-J, Peterkofsky A, Seok Y-J (2007) *Escherichia coli* enzyme IIA<sup>Ntr</sup> regulates the K<sup>+</sup> transporter TrkA. *Proc Natl Acad Sci USA* 104:4124–4129.
- Charpentier B, Bardey V, Robas N, Branlant C (1998) The EIIGlc protein is involved in glucose-mediated activation of *Escherichia coli* *gapA* and *gapB-pgk* transcription. *J Bacteriol* 180:6476–6483.
- Nam T-W, et al. (2001) The *Escherichia coli* glucose transporter enzyme IICB<sup>Glc</sup> recruits the global repressor Mlc. *EMBO J* 20:491–498.
- Decker K, Plumbridge J, Boos W (1998) Negative transcriptional regulation of a positive regulator: The expression of *malT*, encoding the transcriptional activator of the maltose regulon of *Escherichia coli*, is negatively controlled by Mlc. *Mol Microbiol* 27:381–390.
- Kimata K, Inada T, Tagami H, Aiba H (1998) A global repressor (Mlc) is involved in glucose induction of the *ptsG* gene encoding major glucose transporter in *Escherichia coli*. *Mol Microbiol* 29:1509–1519.
- Plumbridge J (1998a) Control of the expression of the *manXYZ* operon in *Escherichia coli*: Mlc is a negative regulator of the mannose PTS. *Mol Microbiol* 27:369–380.
- Plumbridge J (1998b) Expression of *ptsG*, the gene for the major glucose PTS transporter in *Escherichia coli*, is repressed by Mlc and induced by growth on glucose. *Mol Microbiol* 29:1053–1063.
- Kim S-Y, et al. (1999) Purification of Mlc and analysis of its effects on the *pts* expression in *Escherichia coli*. *J Biol Chem* 274:25398–25402.
- Tanaka Y, Kimata K, Inada T, Tagami H, Aiba H (1999) Negative regulation of the *pts* operon by Mlc: Mechanism underlying glucose induction in *Escherichia coli*. *Genes Cells* 4:391–399.
- Plumbridge J (1999) Expression of the phosphotransferase system both mediates and is mediated by Mlc regulation in *Escherichia coli*. *Mol Microbiol* 33:260–273.
- Lee S-J, Boos W, Bouche JP, Plumbridge J (2000) Signal transduction between a membrane-bound transporter, PtsG, and a soluble transcription factor, Mlc, of *Escherichia coli*. *EMBO J* 19:5353–5361.
- Tanaka Y, Kimata K, Aiba H (2000) A novel regulatory role of glucose transporter of *Escherichia coli*: Membrane sequestration of a global repressor Mlc. *EMBO J* 19:5344–5352.
- Eberstadt M, et al. (1996) Solution structure of the IIB domain of the glucose transporter of *Escherichia coli*. *Biochemistry* 35:11286–11292.
- Cai M, et al. (2003) Solution structure of the phosphoryl transfer complex between the signal-transducing protein IIA<sup>Glucose</sup> and the cytoplasmic domain of the glucose transporter IICB<sup>Glucose</sup> of the *Escherichia coli* glucose phosphotransferase system. *J Biol Chem* 278:25191–25206.
- Schiefner A, et al. (2005) The crystal structure of Mlc, a global regulator of sugar metabolism in *Escherichia coli*. *J Biol Chem* 280:29073–29079.
- Jiang S, Tovchigrechko A, Vakser IA (2003) The role of geometric complementarity in secondary structure packing: A systematic docking study. *Protein Sci* 12:1646–1651.
- Seitz S, Lee SJ, Penetier C, Boos W, Plumbridge J (2003) Analysis of the interaction between the global regulator Mlc and EIIB<sup>Glc</sup> of the glucose-specific phosphotransferase system in *Escherichia coli*. *J Biol Chem* 278:10744–10751.
- Seok Y-J, et al. (1997) High affinity binding and allosteric regulation of *Escherichia coli* glycogen phosphorylase by the histidine phosphocarrier protein, HPr. *J Biol Chem* 272:26511–26521.
- Koo B-M, et al. (2004) A novel fermentation/respiration switch protein regulated by enzyme IIA<sup>Glc</sup> in *Escherichia coli*. *J Biol Chem* 279:31613–31621.
- Tanaka Y, Itoh F, Kimata K, Aiba H (2004) Membrane localization itself but not binding to IICB is directly responsible for the inactivation of the global repressor Mlc in *Escherichia coli*. *Mol Microbiol* 53:941–951.
- Xia B, Vlamis-Gardikas A, Holmgren A, Wright PE, Dyson HJ (2001) Solution structure of *Escherichia coli* glutaredoxin-2 shows similarity to mammalian glutathione-S-transferases. *J Mol Biol* 310:907–918.
- Penetier C, Dominguez-Ramirez L, Plumbridge J (2008) Different regions of Mlc and NagC, homologous transcriptional repressors controlling expression of the glucose and N-acetylglucosamine phosphotransferase systems in *Escherichia coli*, are required for inducer signal recognition. *Mol Microbiol* 67:364–377.